A GEO-SPATIAL APPROACH TO RAINFALL VARIABILITY AND TIME SERIES TREND ANALYSIS IN THE MAYURAKSHI BASIN, EASTERN INDIA

David Durjoy Lal Soren, Jonmenjoy Barman, and Brototi Biswas

Department of Geography & RM, Mizoram (Central) University, Aizawl, Mizoram-India
Corresponding Author: devid.dls.king@gmail.com

Abstract

The primary driving forces behind this investigation were the trend in rainfall, variability in change point identification, and forecasting for the Mayurakshi basin, located in eastern India, using the data from 1991 to 2020. Sen's Slope was employed to determine the slope's magnitude, and Mann-Kendall (mMK) statistics were utilized to assess the long-term trend of rainfall. The trend's conclusion showed that the rainfall trend fluctuated throughout time, and then experienced a negative magnitude. The Pettitt Test, the Standard Normal Homogeneity Test (SNHT), and Buishand's U test statistics were used to determine the change point of rainfall during a 30-year long-term period. The results of the change point analysis showed that the significance level was lower than the p-value ($\propto$ = 0.05), indicating a plausible change point in rainfall occurring in the year 2008. To gain insights into the seasonal nature of rainfall, the Rainfall Seasonality Index (RSI) was computed for all rainfall stations in the basin. The RSI indicated equitable rainfall distribution, primarily during the monsoonal season. The assessment of wet and drought conditions in the basin was performed using the Rainfall Anomaly Index (RAI). The RAI revealed that the basin experienced drought in 50% of the years during the 30 years. The outcomes of this study hold practical implications for future planning, including crop and environmental management.

Keywords: Trend; Change point detection; Seasonality; Anomaly.

Introduction

Rainfall is one of the important parameters that directly control water resources and agriculture. For effective management of water resources, accurate quantification of climatic parameters such as rainfall changes is crucial. Water resources are immediately impacted by changes in rainfall patterns, which are directly related to changes in the hydrological cycle (Gajbhiye et al. 2015). The southwest monsoon, which brings copious amounts of precipitation, is extremely important to the Indian subcontinent. However, there has been a rise in precipitation variability and uncertainty in recent decades (Das et al. 2021). Significant spatiotemporal variability and uncertainty in rainfall have been observed across the Indian subcontinent. In contrast to the northeastern region of India, Rajasthan in

western India receives barely 100mm of rain on average each year. Stream flow patterns, soil moisture content, and groundwater recharge are all being impacted by changing climatic conditions, particularly the frequency and amount of rainfall (Srivastava et al. 2014).

The variability and erratic character of rainfall events, which cause longer dry seasons, less runoff, and food insecurity, are the main effects of climate change. As a result, agriculture is greatly impacted by climate change and its effect on rainfall variability in many different places around the world (Gajbhiye et al. 2015). Numerous climate factors have changed as a result of the ongoing increase in fossil fuel use and greenhouse gas emissions. Change points are sudden shifts in climate behaviour. Therefore, it is essential for agricultural planning, and efficient water resource management in any location to analyze climatic factors, notably rainfall patterns, variations, and trends. Understanding precipitation patterns on the Indian subcontinent requires a thorough understanding of climate change.

Numerous studies (Karmeshu et al. 2012) have focused on the evaluation of change points at both global and regional scales. The Mann-Kendall test, Sen's slope non-parametric test, and Pettit's test are frequently used by researchers to evaluate trends, estimate trend magnitudes, and identify change points when they examine historical time series data (Das et al. 2021). To assess the consistency of long-term time series data and spot potential changes, the standard normal homogeneity test is also used (Dhorde et al., 2013).

Various statistical strategies have been utilized for change point detection in the context of parametric methods under the assumption that the data have a normal distribution. According to Chargui et al. (2018), these methods include Buishand U, Buishand range, standard normal homogeneity, and log-likelihood-based approaches. For one to understand climate anomalies and put into practice efficient management techniques, one must have a solid understanding of change detection and trend analysis (Fischer et al. 2012). As a result, understanding rainfall patterns depends heavily on the research of temporal and spatial changes in rainfall as well as the analysis of long-term rainfall time series

The ability to identify trends in climatic variables has been demonstrated by several indexes. The Precipitation Concentration Index (PCI), Rainfall Seasonality Index (RSI), and Rainfall Anomaly Index (RAI) (Walsh and Lawler 1981) are a few examples, these are powerful indicators to understand the behaviour of drought condition seasonal variation in such agrarian Mayurakshi basin. In this study, we concentrate on evaluating rainfall trends and the amplitude of linear changes using Sen's slope and Mann-Kendall statistics. Statistical tests are preferred for determining absolute homogeneity and change points in areas under study that have diverse topographical features or a wide distribution of stations. This is crucial since critical connections might not be readily apparent (Ahmed et al. 2020). Thus, we employed the Pettitt Test, Buishand U Statistic, and Standard Normal Homogeneity Test to identify significant changes in the time series rainfall data.

Additionally, we applied two widely recognized indexes, RSI and RAI, to evaluate the spatio-temporal variability and seasonality of rainfall.

The Mayurakshi River is essential for irrigation, drinking water supply, fishing, and the important agricultural region of eastern India (Ghosh et al. 2022). There are numerous dams and multifunctional projects in the Mayurakshi basin. Several studies conducted on this basin on different aspects such as hydro-geomorphological modification of the Mayurakshi River, and the impact of the Tillpara barrage on the tributary of Mayurakshi (Pal 2016, 2017), spatiotemporal analysis of the regional agricultural disparity of Mayurakshi basin (Chakraborty et al, 2016). The study aims to explore how precipitation affects the Mayurakshi basin. A thorough understanding of rainfall variability and trends will give a comprehensive insight into future patterns, enabling the river basin to plan more efficiently and enhance both agricultural and water resource management planning.

Study area

Mayurakshi is one of the most important river systems in eastern India. The river originates from Trikut Hill in the Chota Nagpur plateau of Jharkhand state. The basin extends from 23° 63′ 12″ to 24° 51′ 3″ N latitude and 86° 84′ 38″ to 88° 16′ 12″ E longitude in the states of Jharkhand and West Bengal and covers an area of 8805.06 km². Geologically, the whole area of the upper part of the basin is dated back to the Proterozoic and Phanerozoic eon formations of undivided Precambrian rock. The middle catchment of the basin is most dominantly deposited by laterite and lateritic soil, and the lower catchment of the basin is mostly covered by young and old alluvial soil. The relief of the upper catchment of the Mayurakshi basin is very undulating and covered with flat-topped isolated hills, most of which are >300 meters. The basin's middle catchment area is part of West Bengal's Birbhum district. It is also known as the Rarh region, and it is part of the undulating eastward-extended fringing portion of the Chotonagpur plateau that ranges from 71m to 120m in height. The lower catchment is mostly covered by the lower-laying flood plain.
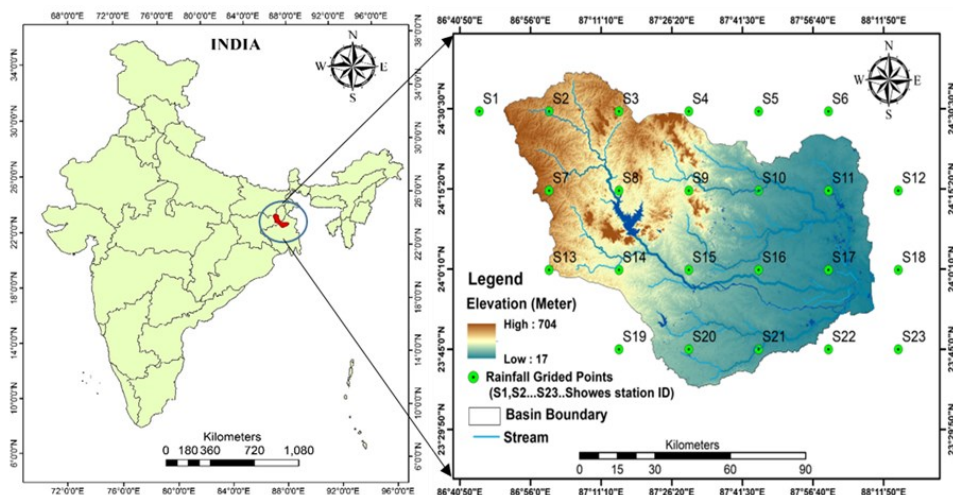

Fig. 1: Location of the study area and distribution of rainfall grid points

Methodology

Data Source

The rainfall data from 1991 to 2020 was collected from the India Meteorological Department (IMD), Pune (https://www.imdpune.gov.in/cmpg/Griddata/Rainfall_25_Bin.html). The obtained daily gridded rainfall data (in millimetres) has a high spatial resolution of 0.25 × 0.25 degrees. After collecting the rainfall data, the row data set was exported to MS Excel, where it was corrected for missing values, and the stations were filtered to get the required rainfall stations for the study area. A total of 23 stations covering the entire study area were assigned names as - S1, S2, S3... S23 (Table 1). The rainfall data was arranged on a daily, monthly, and annual basis for subsequent analysis.

Mann-Kendall Statistic

The Mann-Kendall, a non-parametric test, is a suitable measure for analyzing the trends in time series data, both for long and short-term periods. It assesses consistent increasing or decreasing trends effectively. Due to its non-parametric nature, the MK test can be applied to various data distributions, making it widely used compared to other statistical methods for studying long-term trends in time series data.

The Kendall's statistics (S) in the long-term time series data, denoted as m1, m2, m3, ..., and mn, is estimated using the following equation:

$$S = \sum_{k=1}^{n-1} \sum_{j=k=1}^{n} sgn(x_J - x_k) \qquad \text{(EQ-1)}$$

where sgn (x_J - x_k) is defined as:

$$\left\{ \begin{array}{l} +1 \text{ -------- } (x_J - x_k) > 0 \\ 0 \text{ --------- } (x_J - x_k) = 0 \\ -1 \text{-------- } (x_J - x_k) < 0 \end{array} \right\} \qquad \text{(EQ-2)}$$

In the equation, x1, x2, ..., xn is the data points at different time intervals, where n is the total time period. If the value of n is equal to or greater than 10, a Z-transformation is applied to approximate a normal distribution known as the Kendall Z-value. The Z statistics is obtained by adapting the variance of VAR(S).

$$VAR(S) = 1/18 \left[n(n-1)(2n+5) - \sum_{p-1}^{g} (t_p - 1)(2t_p - 5) \right] \qquad \text{(EQ-3)}$$

Here, n is the number of observations, g is the equal trend values, p represents the value of tide groups in the data set, and tp indicates the number of data values. The symbol Σ represents the summation of all tide groups.

The calculated VAR(S) is employed to compute the Z transformation for the MK test statistics Z-value:

$$Z = \begin{cases} \dfrac{S-1}{VAR(S)} & S > 1 \\ 0, & S = 0 \\ \dfrac{S-1}{VAR(S)} & S < 0 \end{cases} \qquad \text{(EQ-4)}$$

The Z-value follows a standard normal distribution, where the negative value represents a downward trend and the positive value indicates an upward trend. The significance level α is used for testing, typically using a two-tailed test.

Modified Mann–Kendall Test

The statistical test conducted by Kendell can produce inaccurate results when the time series data have a significant autocorrelation. To address this issue, researchers are using the modified Mann-Kendall test. Therefore, before proceeding with the analysis of any time series data, initially the data is tested for serial dependency at the lag-1 significance level. If the data follows a significant autocorrelation in such conditions, modified Mann-Kendall (mMK) statistics were employed.

The mMK VAR (S) is estimated using the following equation:

$$\text{VAR } (S) = \left(\frac{n(n-1)(2n+5)}{18} \right) \cdot \left(\frac{n}{n_e^*} \right) \qquad \text{(EQ-5)}$$

The correction factor $\left(\frac{n}{n_e^*} \right)$ is calculated to adjust the autocorrelation data:

$$\left(\frac{n}{n_e^*} \right) = 1 + \left(\frac{2}{n^3 - 3n^2 + 2n} \right) \sum_{f=1}^{n-1} (n-f)(n-f-1)(n-f-2)\rho_e(f) \qquad \text{(EQ-6)}$$

The value of $\rho_e(f)$ represents the auto-correlation among the rank of observations and is computed as follows:

$$\rho(f) = 2\sin \left(\frac{\pi}{6} \rho_e(f) \right) \qquad \text{(EQ-7)}$$

Sen's Slope

The MK or mMK Statistic is employed to determine the direction (positive or negative) of a given attribute, while Sen's Slope is commonly applied to assess the magnitude of the inclination. Sen (1968) proposed a non-parametric statistic to quantify the slope and measure the linear change. This method, widely employed to compute trend

magnitude (Kamal and Pachauri 2019), utilizes Sen's slope estimates, which can be either positive or negative.

The slope is calculated as described by Hirsch et al. (1982), the equation is as follows:

$$F(t) = Qt+B \qquad \text{(EQ-8)}$$

Here, F(t) represents a time series that can increase or decrease, here Q is the slope and B is a constant. The slope Q can be computed using the formula:

$$Q_i = \frac{xj - xk}{j - k} \quad i = 1,2,3,4,5 \dots n \, j > k \qquad \text{(EQ-9)}$$

In this equation, x_j and xk is the data values at time j and k, consecutively, with j > k. The median of the n values of Qi is determined by the following formula:

$$Qi = \begin{cases} \left[\frac{Qn+1}{2}\right] \dots\dots\dots\dots\dots\dots\dots\dots n \text{ odd} \\ \frac{1}{2}\left[\frac{Qn}{2}\right] + \left[\frac{Qn+2}{2}\right] \dots\dots\dots\dots n \text{ even} \end{cases} \qquad \text{(EQ-10)}$$

The positive Qi represents an increasing trend, whereas a negative Qi represents a decreasing trend, and a value of zero indicates no trend.

Pettitt Test

Pettitt (1997) developed a technique called single change point detection, this statistical analysis is used to identify abrupt changes in time series data. This method has been widely utilized by researchers such as Bryson et al. (2012), and others.

$$U_k = 2\sum_{i=0}^{n} m_i - k(n+1) \qquad \text{(EQ-11)}$$

In Equation 11, m_i presents the order of the ith observation, while x1, x2, x3, ..., xn represent the data points organized in ascending order. The variable k can take values from 1 to n.

$$K = \max |U_k| \qquad \text{(EQ-12)}$$

$$U_k = \sum_{i=1}^{t} \Sigma_{1j=t+1}^{n} sign\,(x_i - x_j) \qquad \text{(EQ-13)}$$

U_k is calculated as the sum of sign (x_i - x_j) for all i from 1 to t, and j from t+1 to n, as shown in Equation 13.

$$K\alpha = [-1n\alpha(n^3 + n^2)/6]^{1/2} \qquad \text{(EQ-14)}$$

To determine the change point in the time series, the value of K come to its maximum at U_k. The critical value, denoted as $K\alpha$, is obtained using Equation 14. Here, α represents the desired level of significance for determining the critical value, and n is the sum of the observations.

Buishand U Statistic

Ndione et al. (2017) employed the Buishand's U test to calculate the change point. This statistical test, proposed by Buishand in 1984, was specifically utilized for detecting a single change point. The formulation of the Buishand U test is expressed as follows:

$$U = \frac{\sum_{k=1}^{n-1}(S_K / D_X)^2}{n(n+1)} \qquad \text{(EQ-15)}$$

In this equation, S_k represents the cumulative deducted value from the mean, and D^2_x corresponds to the standard deviation presented in equations EQ-13 and EQ-14.

$$S_k = \sum_{i=1}^{k}(X_i - \bar{X}) \qquad \text{(EQ-16)}$$

$$D_x^2 = 1/n\sum_{i=1}^{n}(X_i - \bar{X})^2 \qquad \text{(EQ-17)}$$

Standard Normal Homogeneity Test

The standard normal homogeneity (SNH) tests, developed by Alexandersson in 1986, serve as a statistical approach to determine a change point in time-series data. The equations presented by Alexandersson in 1986 are as follows:

$$Ty = y\bar{z}_1 + (n-y)\bar{z}_2, Y = 1.2, 3........n \qquad \text{(EQ-18)}$$

In Equation 18, the $T_{(y)}$ statistic is computed to compare the mean value of the first year (y) and the last year (n-y). The computation of Z1 and Z2 can be expressed as follows:

$$\bar{Z}_1 = 1/y\sum_{i=1}^{n}(y_1 - \bar{y}/S_q) \text{ and } \bar{Z}_2 = 1/n-y\sum_{i=y+1}^{n}(y_1 - \bar{y}/S_q) \qquad \text{(EQ-19)}$$

In Equation 19, represents the arithmetic mean of the ratio S_q, while represents the standard deviation of the series. A breaking point within the time series is identified when the *T* value reaches its maximum. The homogeneity critical value is computed to determine the homogeneity.

$$T_o = \max T_y \qquad \text{(EQ-20)}$$

Rainfall Seasonality Index

The Rainfall Seasonality Index (RSI) is a measurement which conveys the relative seasonality of the rainfall pattern. RSI is the statistical representation of the annual discrepancy in monthly rainfall. RSI helps in understanding the seasonal characteristics of rainfall and its pattern. The RSI is calculated using the following formula (Walsh and Lawler, 1981):

$$RSI = \frac{1}{\bar{R}} \sum_{n=1}^{n=12} \left| \bar{x}_{ny} - \bar{R}_y / 12 \right| \qquad \text{(EQ-21)}$$

n the formula, $\bar{x}_{ny}$ indicates the calculated rainfall in month n of a given year y, while $\bar{R}_y$ / 12 indicates the average yearly rainfall for that particular year ᵧ.

Rainfall Anomaly Index

This study computed the precipitation abnormalities using the statistical method known as the Rainfall Anomaly Index (RAI). Indicating deviations from typical rainfall quantities, anomalies can be either positive (+) or negative (-). Following the method suggested by Van-Rooy (Van-Rooy 1965), the ten highest and lowest precipitation measurements are ordered and averaged to create thresholds for positive and negative anomalies.

The RAI is computed using the following equations:

$$RAI = 3 * (Pi - \bar{P}) / (\bar{r} - \bar{P}) \qquad \text{(EQ-22)}$$

$$RAI = -3 * (Pi - \bar{P}) / (\bar{r} - \bar{P}) \qquad \text{(EQ-23)}$$

Here, Pi stands for the annual precipitation in millimeters, P for the time series' average rainfall, and (r, P) for the average of the ten highest and lowest annual precipitation values. The prefix ±3 is used to calculate positive and negative anomalies, respectively.

Results and Discussion

Rainfall Dynamics

To examine the evolving patterns and spatial-temporal fluctuations of rainfall, an analysis was conducted using the comprehensive rainfall data of the Mayurakshi basin spanning from 1991 to 2020. The study encompassed 23 rainfall stations situated within the basin. Below is a summary of the decadal annual and seasonal variations in rainfall as well as the long-term trend in rainfall variability.

Decadal and long-term variation of rainfall

The focus of the study was a 30-year span of rainfall variations, examining spatial and seasonal patterns at a micro-level scale. In the first decade (1991–2000), rainfall

exhibited a consistent upward trend (Fig. 3). The characteristics of rainfall in this period varied, ranging from a maximum and minimum of 1964.86 mm and 1288.99 mm to an average of 1557.10 ± 174.44 mm. The upper part of the basin experienced a significant concentration of rainfall. Moving into the second decade, the mean annual rainfall was 1430.30 ± 155.26 mm, displaying lower variability (CVR 10.85) compared to the first and third decades (Table 1). Between 2001 and 2010, the northeast region of the upper and middle basin areas observed a high concentration of rainfall (Fig. 4b). However, in the third decade, the basin received lower rainfall (1438.68 mm) compared to the first and second decades. During this period, the maximum and minimum rainfall were recorded as 1438.68 mm and 989.27 mm, respectively, with an average of 1207.24 ± 138.41 mm. Rainfall in the third decade displayed a decreasing trend from the upper to the middle and lower basin areas (Fig. 2c). Overall, in the long-term rainfall pattern, the maximum and minimum rainfall of the basin were 1717.37 mm and 1172.51 mm, respectively, with an average annual rainfall of 1398.21 ± 139.95 mm. The northeastern regions of the upper and middle basin areas consistently experienced a high concentration of rainfall, while the lower parts of the basin generally recorded low rainfall over the study period (Table 1, Fig. 2d). Geographically, the upper part of the basin is located in a plateau region, with plateau mountains contributing to favourable conditions for monsoonal rainfall. This explains the higher rainfall that occurred in the upper basin than in the lower basin area.
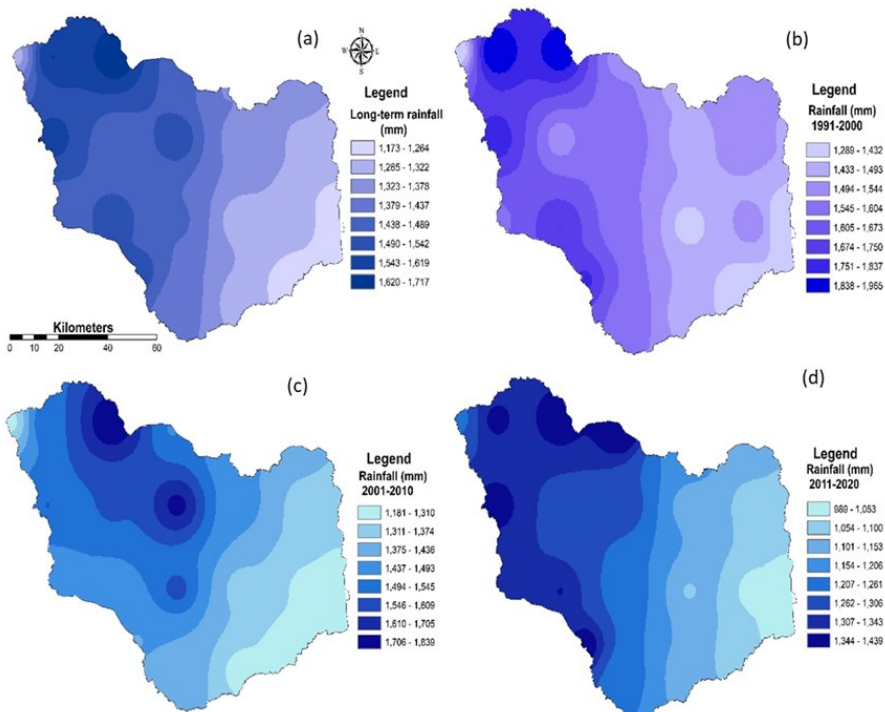

Fig. 2: Decadal and long-term spatial rainfall variation (a) 1st decade, (b) 2nd decade, (c) 3rd decade, (d) long-term basin average

Table 1: Decadal and long-term rainfall variation

Latitude	Longitude	Station	Rainfall (mm)			
			1991-2000	2001-2010	2011-2020	Long-term
24.5	86.75	**S1**	1366.99	1281.24	1243.97	1297.40
24.5	87.00	**S2**	1964.86	1539.25	1355.59	1619.90
24.5	87.25	**S3**	1932.73	1838.98	1380.41	1717.37
24.5	87.50	**S4**	1517.00	1490.56	1438.68	1482.08
24.5	87.75	**S5**	1473.01	1463.85	1188.43	1375.10
24.5	88.00	**S6**	1531.51	1405.81	1152.86	1363.39
24.25	87.00	**S7**	1803.64	1544.97	1369.27	1572.63
24.25	87.25	**S8**	1503.83	1553.95	1297.35	1451.71
24.25	87.50	**S9**	1577.24	1744.03	1305.31	1542.20
24.25	87.75	**S10**	1456.03	1459.32	1117.93	1344.42
24.25	88.00	**S11**	1533.84	1336.77	1058.22	1309.61
24.25	88.25	**S12**	1485.60	1320.04	1061.23	1288.96
24.00	87.00	**S13**	1589.06	1446.53	1340.73	1458.77
24.00	87.25	**S14**	1750.35	1465.52	1344.43	1520.10
24.00	87.50	**S15**	1550.16	1566.56	1237.19	1451.30
24.00	87.75	**S16**	1391.20	1345.04	1095.81	1277.35
24.00	88.00	**S17**	1541.70	1287.93	1028.08	1285.90
24.00	88.25	**S18**	1288.99	1232.09	996.44	1172.51
23.75	87.25	**S19**	1770.11	1435.10	1377.65	1527.62
23.75	87.50	**S20**	1583.93	1413.80	1220.77	1406.16
23.75	87.75	**S21**	1459.81	1271.42	1106.56	1279.26
23.75	88.00	**S22**	1325.02	1180.60	1060.33	1188.65
23.75	88.25	**S23**	1416.67	1273.55	989.27	1226.49
maximum			1964.86	1838.98	1438.68	1717.37
minimum			1288.99	1180.60	989.27	1172.51
average			1557.10	1430.30	1207.24	1398.21
SD			174.44	155.26	138.41	139.95
CVR			11.20	10.85	11.46	10.00

Trend of rainfall

The modified Mann-Kendall (mMK) statistic was employed to assess the trend over a 30-year period within the basin. The comprehensive analysis of the entire basin using the mMK indicated variations in rainfall and the impact of climate change throughout the study period. The p-value was computed to determine the overall rainfall variation, and it was

found to be less than the significance level alpha (0.05), suggesting a plausible change in the basin's rainfall series during the 30-year period. Additionally, the trend exhibited temporal variability.

In general, the negative Kendall's Z value (-1.67) and normalized Kendall's tau (-0.218) indicated a decreasing trend in rainfall (Fig 3 and Table 2). Furthermore, Sen's slope, which provides a measure of the trend's magnitude, showed a strongly negative value (-10.40), indicating a downward trend in rainfall (Fig 3). The basin comprised 23 rainfall stations, and except for station S8, all stations exhibited negative rainfall trends throughout the sampled period. Among them, stations S2, S17, S11, S12, S23, and S24 demonstrated the highest negative Sen's slope values (Q = -25.77, -21.30, -19.48, -18.20, -18.15, and -17.20), signifying a significant decline in rainfall trends. Correspondingly, these stations also exhibited negative Z statistics of -2.18, -5.00, -4.02, -3.39, -2.85, and -2.00, respectively.

Within the study area, significant negative rainfall trends were recorded at S2, S6, S10, S11, S12, S17, S20, and S23, with consistent patterns of negative normalized Kendall's Z and Sen's slope Q values (Fig 4 and Table 2).
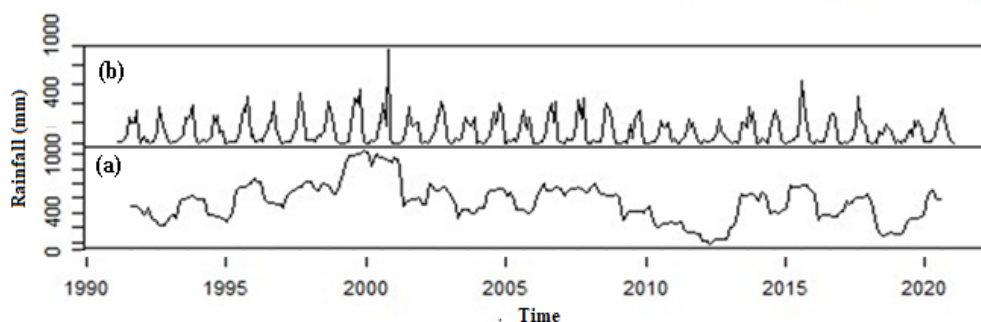

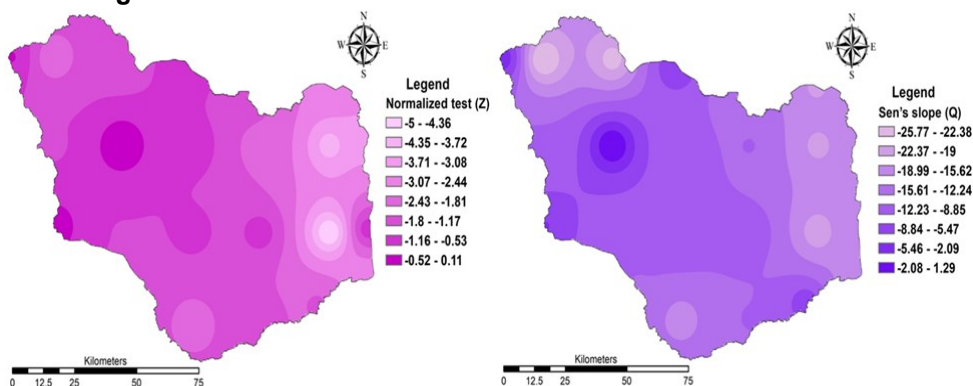**Fig. 3: Rainfall trend with seasonal and random variation**

Fig 4: Normalized Z (a) Sen's slope Q (b)

Table 2: Modified Mann Kendall Statistic and Sen's slope estimation

Station	Normalized Test (Z)	Kendall's tau	p-value (Two-tailed)	Sen's slope (Q value)
Basin	-1.67	-0.218	0.035	-10.40
S1	-0.50	-0.070	0.617	-3.980
S2	-2.18	-0.280	0.030	-25.77
S3	-1.70	-0.200	0.089	-23.71
S4	-0.61	-0.089	0.538	-6.020
S5	-1.25	-0.195	0.211	-14.20
S6	-2.68	-0.347	0.007	-19.39
S7	-1.23	-0.200	0.219	-12.14
S8	0.11	0.020	0.91	1.300
S9	-0.69	-0.100	0.492	-10.68
S10	-2.09	-0.241	0.036	-12.11
S11	-4.02	-0.356	<0.05	-19.84
S12	-3.39	-0.301	<0.05	-18.20
S13	-0.21	-0.030	0.830	-5.400
S14	-1.18	-0.150	0.239	-10.07
S15	-0.89	-0.140	0.374	-9.230
S16	-0.86	-0.110	0.392	-9.700
S17	-5.00	-0.370	<0.05	-21.30
S18	-0.86	-0.154	0.388	-15.95
S19	-1.64	-0.210	0.101	-12.37
S20	-2.00	-0.260	0.046	-17.20
S21	-1.61	-0.210	0.108	-12.18
S22	-1.74	-0.150	0.083	-6.880
S23	-2.85	-0.370	0.004	-18.15

Change point of annual rainfall

Various statistical methods, including Pettitt's, SNHT, and Buishand's U tests, were utilized to identify the homogeneity and change points in rainfall patterns. These tests confirmed that a braking point or change point occurred in 2008. Bera et al (2021) stated drought condition extended in the part of Chhota Nagpur Plateau due to low precipitation caused by drastic land use land cover change and modification of cropping pattern. Sankar et al (2023) studied the mining activity of Jharkhand mining area, where the coal mining is the reason of black carbon concentration. Their statistical teste resulted a negative correlation of black carbon mass concentration with rainfall, all of these factors are the

cause of negative trend of rainfall with its step change encountered in 2008. The mathematical models employed in the analysis revealed that the computed p-value, with a confidence interval of 95%, was below the significance level ($\propto$ = 0.05), indicating a notable change in rainfall over the 30-year study period. Concerning individual rainfall stations, the models demonstrated significant breakpoints in annual rainfall at stations S3, S14, S15, S20, and S23 in 2008, at S2 in 2007, and at stations S10, S11, and S12 in 2009. These breakpoints occurred approximately in the middle of the observation period (Table 3). On the other hand, when applying the change-point models (Pettitt's test, SNHT test, Buishand's U test), the calculated p-value exceeded the significance level ($\propto$ = 0.05) at the 95% of confidence interval for 52.17% of the stations (S1, S4, S5, S7, S8, S9, S13, S16, S18, S19, S21, S22). This result indicates that there were no significant changes in rainfall throughout the study period at those particular stations.

Table 3: Change point statistics of the basin

Station	Pettitt's test			SNHT test			Buishand's U test		
	U	t	p 95%	T0	t	P 95%	Q	t	P 95%
Basin	124	2008	0.043	7.395	2008	0.046	0.508	2008	0.032
S1	95	2007	0.287	4.502	2007	0.325	0.226	2007	0.225
S2	153	2007	0.013	10.269	2007	0.012	0.809	2007	0.004
S3	154	2008	0.012	10.045	2008	0.013	0.594	2008	0.020
S4	790	2017	0.522	5.792	2017	0.174	0.107	2017	0.559
S5	124	2008	0.073	7.523	2009	0.067	0.502	2008	0.033
S6	151	2009	0.014	10.291	2009	0.011	0.800	2009	0.004
S7	114	2008	0.122	4.295	2008	0.362	0.286	2008	0.151
S8	940	1996	0.299	4.809	1996	0.285	0.240	2008	0.201
S9	120	2008	0.090	6.378	2008	0.130	0.321	2008	0.114
S10	155	2009	0.011	10.591	2009	0.009	0.591	2009	0.019
S11	153	2009	0.013	10.597	2009	0.008	0.851	2009	0.003
S12	141	2009	0.027	9.338	2009	0.023	0.721	2009	0.008
S13	78	2008	0.541	3.443	2008	0.525	0.248	2008	0.188
S14	116	2008	0.011	5.855	2008	0.167	0.472	2008	0.010
S15	136	2008	0.037	7.599	2008	0.041	0.406	2008	0.046
S16	107	2019	0.171	4.781	2009	0.293	0.284	2009	0.156
S17	148	2002	0.018	9.995	2009	0.014	0.846	2009	0.002
S18	98	2008	0.253	6.791	1994	0.104	0.349	2008	0.097
S19	118	2008	0.100	5.347	2000	0.218	0.366	2000	0.082
S20	140	2008	0.030	7.872	2008	0.054	0.540	2008	0.027
S21	140	2008	0.195	4.801	2008	0.285	0.393	2008	0.070
S22	90	2002	0.350	3.497	2002	0.510	0.263	2002	0.169
S23	152	2008	0.013	8.720	2008	0.031	0.651	2008	0.011

Rainfall seasonality index

The study examined the long-term rainfall patterns in the basin, focusing on individual stations over a 30-year period. The objective was to understand the seasonality of rainfall in the basin. The analysis revealed two predominant classes of Rainfall Seasonality Index (RSI) across the basin: "Very equable" (RSI < 0.19) and "Equable indefinite weather" (RSI between 0.20 and 0.39). When considering the entire 30-year period, 60% of the sampled years exhibited very equal rainfall, while the remaining 40% had equable indefinite weather, which is characteristic of monsoonal rainfall.

Further examination of individual stations (S4, S5, S6, S12, S17, S18, S21, and S23) showed that 60% of the sampled years had consistently equitable rainfall throughout the year. At 52.17% of the stations (S1, S2, S3, S8, S9, S10, S11, S14, S16, S19, S20, and S22), the RSI indicated very equitable and equitable definite weather in 50.00% or more of the sampled years. The decadal analysis of the basin's rainfall seasonality confirmed an equitable pattern.

Spatially, the upper basin experienced higher rainfall intensities with RSI values between 0.20 and 0.39 during the first and second decades. In the third decade, the southern part of the middle and lower basins had RSI values above 0.20. The study area predominantly receives monsoonal rain, and the upper and middle basins exhibit similar rainfall characteristics due to their plateau location and orographic conditions. However, in the lower basin area, which consists of the plain region of the basin, there is a notable difference between very equable and equable definite weather rainfall. On average, 56.67% of the sampled years had very equable rainfall, while 43.33% had equable definite weather rainfall. This disparity may be attributed to the absence of a topographic barrier, leading to increased rainfall uncertainty in the region.

The focal region, primarily encompassing portions of Jharkhand and West Bengal, is chiefly characterized by the presence of the Mayurakshi and Dwarka rivers. Agriculture in this area relies heavily on rainfall and is predominantly mono-crop oriented, resulting in noticeable disparities across different agricultural regions (Chakraborty et al, 2016). Given the significant reliance on rainfall for agricultural activities, analysing the Rainfall Sensitivity Index (RSI) over decades and observing its spatiotemporal variations proves to be a valuable approach for crop selection and mitigating inter-regional agricultural imbalances.

Rainfall anomaly index

The evaluation of the dry and rainy conditions in the basin was conducted based on the Rainfall Anomaly Index (RAI). Over a span of 30 years, the temporal patterns of rainfall were analyzed, revealing that 6.67% of the years were extremely wet, while 16.67%, 13.33%, 6.67%, 13.33%, and 3.33% of the sampled years fell into the categories of very wet, moderately wet, slightly wet, near normal, and slightly dry, respectively. Additionally, 16.67% of the years were identified as extremely dry across the basin.

The spatiotemporal analysis of RAI indicated that 13.33% of the years exhibited extremely wet conditions (>3.00) at 47.83% of the stations (S1, S3, S5, S7, S9, S12, S17, S18, S20, S21). Moreover, extremely dry conditions (<-3.00) were observed in 13.33% of the years at stations S1, S7, S8, S10, S11, S12, S15, S16, S17, S19, and S20 throughout the basin. Very wet conditions were recorded in 13.33% of the years at stations S2, S5, S20, and S25, whereas 10.00% of the years were classified as very wet at stations S6, S8, S10, S12, S15, and S17. The moderately wet condition of RAI was observed in 16.67% of the years across 30.43% of the stations.

Table 4: Rainfall seasonality and decadal status

Station	RSI Class (Year in percent)		RSI decadal average		
	Very equable (<0.19)	Equable in definite weather (0.20-0.39)	1991-2000	2001-2010	2011-2020
Basin	60.00	40.00	0.19	0.19	0.22
S1	50.00	50.00	0.23	0.20	0.24
S2	50.00	50.00	0.22	0.20	0.23
S3	50.00	50.00	0.20	0.20	0.22
S4	60.00	40.00	0.20	0.17	0.22
S5	60.00	40.00	0.20	0.16	0.22
S6	60.00	40.00	0.19	0.19	0.21
S7	46.67	53.33	0.22	0.21	0.24
S8	56.67	43.33	0.20	0.23	0.20
S9	53.33	46.67	0.21	0.21	0.21
S10	56.66	43.33	0.20	0.20	0.21
S11	56.66	43.33	0.20	0.19	0.22
S12	60.00	40.00	0.19	0.18	0.22
S13	46.67	53.33	0.21	0.22	0.24
S14	50.00	50.00	0.19	0.22	0.23
S15	46.67	53.33	0.20	0.21	0.24
S16	50.00	50.00	0.20	0.19	0.24
S17	60.00	40.00	0.20	0.19	0.22
S18	60.00	40.00	0.21	0.17	0.21
S19	50.00	50.00	0.20	0.20	0.24
S20	53.33	46.67	0.20	0.20	0.24
S21	60.00	40.00	0.20	0.18	0.23
S22	56.67	43.33	0.21	0.19	0.22
S23	63.33	36.66	0.20	0.18	0.21

Among the 23 rainfall stations, the highest occurrence of near normal conditions was found in 26.67% of the years at stations S16 and S19, and in 20.00% of the years at stations S6 and S9. On the other hand, the least frequent near normal condition, accounting for 3.33% of the counted years, was observed at stations S4, S5, S8, and S12. The very dry condition of RAI was prevalent in 23.33% of the years at station S9 and in 20.00% of the years at stations S8 and S19. Similarly, a moderately dry classification was assigned to 13.33% of the years at stations S1, S5, S13, S16, S19, and S21. Overall, the basin experienced a total drought condition in 46.67% of the years, with S2 and S15 being the most affected stations, accounting for 60.00% and 53.33% of the drought years, respectively, among 20.00% of the stations (S1, S3, S7, S16, S19, and S20) (Table 5).
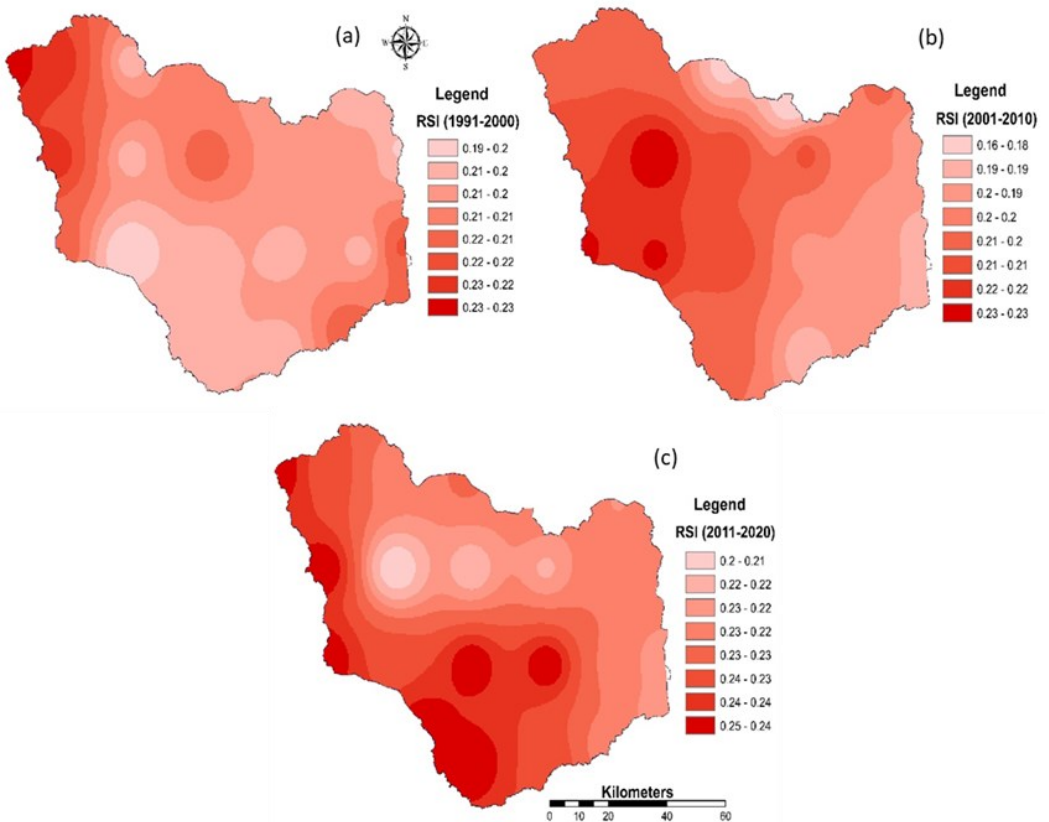

Fig .5: RSI decadal average (a) 1ˢᵗ decade, (b) 2ⁿᵈ decade, (c) 3ʳᵈ decade

In terms of spatiotemporal variation, the RAI analysis indicated that the years from 2008 to 2014 were characterized by extreme drought conditions, while the period from 1996 to 2001 experienced extreme wet conditions for the basin (Fig 6: Basin). Specifically, S1, S3, S5, and S8 recorded a continuous period of extreme wet conditions from 1997 to 2003. The initial years were predominantly classified as drought years at stations S1, S2, S3, S4, S5, S7, S13, S14, S15, S16, S18, S19, and S20 (Fig 6).
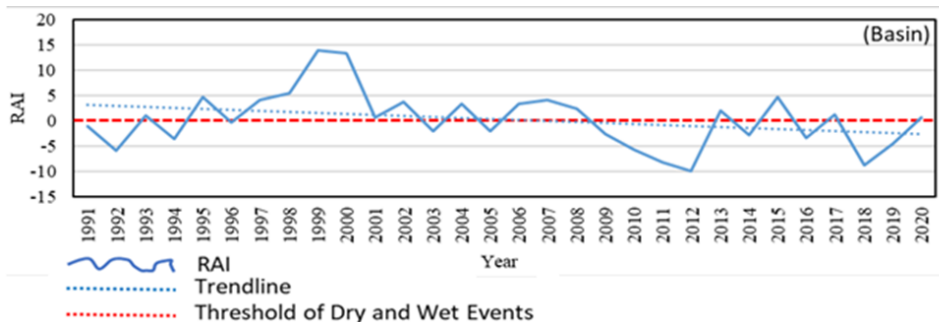
Fig. 6: RAI of the basin

Table 5: Rainfall anomaly and drought status

Station	Extremely Wet >3.00	Very Wet 2.00 to 2.99	Moderately Wet 1.00 to 1.99	Slightly Wet 0.50 to 0.99	Near Normal 0.49 to -0.49	Slightly Dry -0.50 to -0.99	Moderately Dry -1.00 to -1.99	Very Dry -2.00 to -2.99	Extremely Dry <-3.00	Drought year (%)
Basin	6.67	16.67	13.33	6.67	13.33	3.33	20.00	3.33	16.67	46.67
S1	13.33	6.67	13.33	13.33	0.00	13.33	13.33	13.33	13.33	53.33
S2	10.00	13.33	6.67	6.67	10.00	10.00	20.00	6.67	16.67	60.00
S3	13.33	6.67	20.00	6.67	6.67	0.00	16.67	10.00	20.00	53.33
S4	16.67	0.00	16.67	20.00	3.33	0.00	13.33	13.33	16.67	46.67
S5	13.33	13.33	16.67	10.00	3.33	10.00	10.00	6.67	16.67	46.67
S6	16.67	10.00	6.67	6.67	20.00	6.67	6.67	6.67	20.00	46.67
S7	13.33	0.00	10.00	23.33	0.00	3.33	20.00	16.67	13.33	53.33
S8	10.00	10.00	13.33	10.00	3.33	3.33	16.67	20.00	13.33	56.67
S9	13.33	6.67	3.33	10.00	20.00	10.00	3.33	23.33	10.00	56.67
S10	16.67	10.00	10.00	6.67	16.67	10.00	10.00	6.67	13.33	46.67
S11	16.67	6.67	16.67	10.00	10.00	3.33	20.00	3.33	13.33	50.00
S12	13.33	10.00	16.67	16.67	3.33	0.00	23.33	3.33	13.33	40.00
S13	10.00	6.67	10.00	10.00	13.33	3.33	13.33	16.67	16.67	56.67
S14	10.00	6.67	10.00	10.00	13.33	10.00	10.00	13.33	16.67	50.00
S15	13.33	10.00	16.67	0.00	0.00	20.00	16.67	10.00	13.33	60.00
S16	10.00	6.67	16.67	3.33	26.67	0.00	13.33	10.00	13.33	53.33
S17	13.33	10.00	20.00	6.67	6.67	6.67	20.00	3.33	13.33	50.00
S18	13.33	6.67	16.67	6.67	20.00	3.33	3.33	13.33	16.67	50.00
S19	10.00	3.33	13.33	0.00	23.33	3.33	13.33	20.00	13.33	53.33
S20	13.33	13.33	10.00	6.67	10.00	6.67	16.67	10.00	13.33	53.33
S21	13.33	6.67	13.33	13.33	16.67	6.67	13.33	6.67	10.00	46.67
S22	10.00	6.67	23.33	3.33	13.33	13.33	20.00	0.00	10.00	46.67
S23	10.00	13.33	20.00	10.00	6.66	10.00	6.66	6.66	16.67	40.00

Conclusion

The study was aimed at analyzing the spatiotemporal characteristics of rainfall in the Mayurakshi basin. The findings of long-term rainfall revealed that the upper and middle regions of the basin received the highest rainfall concentrations, ranging from 1500 to 1700 mm, where the maximum and minimum rainfall were recorded as 1717.37 mm and 1172.51 mm, respectively, with a mean annual rainfall of 1398.21 ± 139.95 mm. The upper and

middle areas consistently experienced a significant concentration of rainfall over the long term, while the lower parts of the basin exhibited lower rainfall levels. Statistical analysis, including Kendall's Z test (-1.67), normalized Kendall's tau (-0.218), and Sen's slope value (-10.40), indicated a decreasing trend in rainfall within the basin. Decadal rainfall patterns also indicated a declining nature of rainfall across the basin. To assess the homogeneity and identify the change point of rainfall, statistical tests such as Pettitt's test, the SNHT test, and Buishand's test were employed. The results revealed that the change point occurred in 2008. The Rainfall Anomaly Index (RAI) computed the temporal characteristics of rainfall that were classified as extremely wet (6.67% of the years), very wet (16.67%), moderately wet (13.33%), slightly wet (6.67%), slightly dry (3.33%), and extremely dry (16.67%) across the basin. As previous studies stated, the region is facing an inter-regional imbalance in agricultural development, and the region depends on rainfall for a mono-crop cultivation system. Thus, this rainfall trends its nature (RSI, RAI), and micro-level information obtained from this study will provide valuable insights for crop selection and water resource planning. These findings will aid planners and scientists in crop intensity development, the measures of diverse agricultural indices with emphasis on eradicating regional imbalance in crop management and regional planning to ensure efficient water resource utilization in the basin.

Data availability statement: Data will be made available from the corresponding author on reasonable request.

References

1. Ahmad, A., Tang, D., Wang, T. F., Wang, M., & Wagan, B. (2014). Precipitation Trends over Time Using Mann-Kendall and Spearman's rho Tests in Swat River Basin, Pakistan. *Hindawi Publishing Corporation Advances in Meteorology*, 1-16. doi:http://dx.doi.org/10.1155/2015/431860

2. Alexandersson, H. (1986). A Homogeneity Test Applied to Precipitation Data. *Journal of Climatology, 6*(6), 661-675. doi:https://doi.org/10.1002/joc.3370060607.

3. Bera,B., Shit, P.K., Sengupta, N., Saha, S., Bhattacharjee, S. (2021). Trends and variability of drought in the extended part of Chhota Nagpur plateau (Singbhum Protocontinent), India applying SPI and SPEI indices. *Environmental Challenges*.1-10. https://doi.org/10.1016/j.envc.2021.100310

4. Bryson, C., Richard, E., & Adrian, W. (2012). Trend estimation and change point detection in individual climatic series using flexible regression methods. (Vol. 117:D16106.). *J Geophys Res.* doi:doi:10.1029/2011JD017077

5. Buishand, T. (1984). Test for Detecting a Shift in the Mean of Hydrological Time Series (Vol. 73). *Journal of Hydrology.* doi:https://doi.org/10.1016/0022-1694(84)90032-5

6. Chargui, S., Jaberi, A., Cudennec, C., Lachaal, F., Calvez, R., & Slimani, M. (2018). Statistical detection and no-detection of rainfall change trends and breaks in semiarid Tunisia— 50+ years over the Merguellil agro-hydro-climatic reference basin. *Arabian Journal of Geosciences*, 1-14. doi:https://doi.org/10.1007/s12517-018-4001-9

7. *Chakraborty, s., Ghosh, S. (2016). Regional Disparity in The Perspective Of Agricultural Development – A Spatio-Temporal Analysis, Ajay-Mayurakshi Interfluve, Birbhum District, West Bengal, India. IOSR Journal of Economics and Finance.* 43-50

8. Das, J., Mandal, T., Rahman, A. S., & Saha, P. (2021). Spatio-temporal characterization of rainfall in Bangladesh: an innovative trend and discrete wavelet transformation approaches. *Theoretical and Applied Climatology*. doi:https://doi.org/10.1007/s00704-020-03508-6

9. Fischer, T., Gemmer, M., Liu, L., & Su, B. (2012). Change-points in climate extremes in the Zhujiang River basin, South China, 1961–2007. *Climatic Change, 110*, 783–799. doi:https://doi.org/10.1007/s10584-011-0123-8

10. Gajbhiye, S., Meshram, C., Singh, S. K., Srivastava, P. K., & Islam, T. (2015). Precipitation trend analysis of Sindh River basin, India, from 102-year record (1901–2002). *Atmospheric Science Letters, 17*(1), 71-77.

11. Ghosh, S., Sarkar, B., Islam, A., & Shit, P. K. (2022). Assessing the Suitability of Surface Water and Groundwater for Irrigation Based on Hydro-chemical Analysis: A Study of the Mayurakshi River Basin, India. *Air, Soil & Water Research*, *15*.

12. Hamed, K. H., & Rao, A. R. (1998). A modified Mann-Kendall trend test for autocorrelated data. *Journal of Hydrology, 204*(1-14), 182-196. doi: https://doi.org/10.1016/S0022-1694(97)00125-X

13. Hirsch, R. M., Slack, J. R., & Smith , R. A. (1982). Techniques of trend analysis for monthly water quality data. *Water Resources Research, 18*(1), 107-121. doi: https://doi.org/10.1029/WR018i001p00107

14. Islam, A., Barman, S. D., Islam, M., & Ghosh, S. (2020). Role of human interventions in the evolution of forms and processes in the Mayurakshi River Basin. *Anthropogeomorphology of Bhagirathi-Hooghly river system in India*, pp. 135-187. https://doi.org/10.1201/9781003032373

15. Karmeshu, N. (2012). Trend Detection in Annual Temperature and Precipitation using the Mann Kendall Test—A Case Study to Assess Climate Change on Select States in the Northeastern United States. *Master of Environment Studies Capstone project, University of Pennsylvania USA*. Retrieved from http://repository.upenn.edu/mes_capstones/47

16. Kamal, N., & Pachauri, S. (2019). *Mann-Kendall, and Sen's Slope estimators for precipitation trend analysis in north-eastern states of India* (Vol. 177). International Journal of Computer Applications.

17. Ndione, D. M., Sambou, S., Sane, M. L., Kane, S., Leye, I., Tamba, S., & Cisse, M. T. (2017). *Statistical Analysis for Assessing Randomness, Shift and Trend in Rainfall Time*

Series under Climate Variability and Change: Case of Senegal (Vol. 5). Journal of Geoscience and Environment Protection. doi:DOI: 10.4236/gep.2017.513003

18. Pal, S. (2016). Impact of Massanjore Dam on hydro-geomorphological modification of Mayurakshi River, Eastern India. *Environ Dev Sustain, 18*, 921-944. doi:DOI 10.1007/s10668-015-9679-1

19. Pal, S. (2017). Impact of Tilpara barrage on backwater reachof Kushkarni River: a tributary of Mayurakshi River, *Environ Dev Sustain,* 19:2115–2142 *DOI 10.1007/s10668-016-9833-4*

20. Pettitt, A. N. (1997). A Non-Parametric Approach to the Change-Point Problem. *Journal of the Royal Statistical Society. Series C (Applied Statistics), 28*(2), 126-135. . doi:https://doi.org/10.2307/2346729

21. Sarkar, T.K., Ambade, B., Mahato, D.K., Kumar, A., Jangde, R. (2023). Anthropogenic fine aerosol and black carbon distribution over urban environment. Umm Alqura University.472-480.

22. Sen, P. (1968). *Estimates of the regression coefficient based on Kendall's tau* (Vol. 63). Journal of the American Statistical Association.

23. Srivastava, P. K., Han, D., Rico-Ramirez, M. A., & Islam, T. (2014). Sensitivity and uncertainty analysis of mesoscale model downscaled hydro-meteorological variables for discharge prediction. *Hydrological Processes, 28*, pp. 4419–4432.

24. Van-rooy, M. (1965). A Rainfall Anomaly Index (RAI), Independent of the Time and Space. *Notos, 14*, 43-48.

25. Walsh, R., & Lawle, D. (1998). RAINFALL SEASONALITY: DESCRIPTION, SPATIAL PATTERNS AND CHANGE THROUGH TIME. *Department of Geography, University College of Swansea, Department of Geography, University of Birmingham*, 201-208.